# Benzo[*a*]aceanthrylene Derivatives for Red-Emitting Electroluminescent Materials

Tai-Hsiang Huang,[†] Jiann T. Lin,*[,†,‡] Yu-Tai Tao,*[,†] and Chang-Hao Chuen[†]

*Institute of Chemistry, Academia Sinica, 115 Nankang, Taipei, Taiwan and Department of Chemistry, National Central University, 320 Chungli, Taiwan*

*Received July 15, 2003. Revised Manuscript Received October 2, 2003*

Benzo[*a*]aceanthrylene-cored compounds (**acen**) encapsulated with two peripheral arylamines have been synthesized from 1-chloro-anthraquinone by the method of Dehaen, palladium-catalyzed aromatic C−N coupling reactions, and cyclization of diphenylanthracene. These compounds have high thermal stability, and they readily form glass with high glass-transition temperatures. The emission colors of the compounds vary from orange to red. Two quasi-reversible one-electron oxidation waves were observed for the two peripheral amines which are in different chemical environments. The new materials can be deposited as a pure thin film. Pure red-emitting devices were fabricated using **acen** as both hole-transporting and emitting materials and 1,3,5-tris(*N*-phenylbenzimidazol-2-yl)benzene (TPBI) as the electron-transporting materials, or using $Alq_3$ (tris(8-hydroxyquinoline)aluminum) as the electron-transporting materials interposing a hole-blocking BCP layer between **acen** and $Alq_3$.

## Introduction

There has been enormous interest and many research activities in organic light-emitting diodes (OLEDs) since the reports of Kodak's[1] team and Cambridge's[2] group on small molecule-based and polymer-based devices, respectively. Application of OLEDs in flat panel displays and portable electronic devices has become realizable because of considerable progress in organic electroluminescence (EL) materials and devices. Among blue-, green-, and red-emitting materials required for a full-color display, high-performance materials that emit red light of high brightness and color fidelity are rarer.[3] The most commonly used red-emitters include pyran-containing compounds,[4] porphyrin derivatives,[5] europium[6] and *d*-block metal[7] chelate complexes, and fused aromatic compounds.[8] These molecules have a great tendency to aggregate because of their strong charge-transfer (CT) character or flat conjugated structure. Such an outcome generally results in fluorescence quenching. Consequently, the aforementioned red emitters are best applied as dopants in appropriate hosts. Careful control of the dopant concentration is very critical in these devices. Insufficient doping concentration results in loss of color fidelity due to insufficient carrier trapping of the guest or incomplete energy transfer from the host. On the other hand, higher doping concentration often leads to serious concentration quenching, wavelength shift, and decline of EL efficiency.[4b,8a]

* Authors to whom correspondence should be addressed. Fax: Int. code +(2)27831237. E-mail: jtlin@chem.sinica.edu.tw.

† Academia Sinica.

‡ National Central University.

(1) Tang, C. W.; VanSlyke, S. A. *Appl. Phys. Lett.* **1987**, *51*, 913.

(2) Burroughes, J. H.; Bradley, D. D. C.; Brown, A. R.; Marks, R. N.; MacKay, K.; Friend, R. H.; Burn, P. L.; Holmes, A. B. *Nature* **1990**, *347*, 359.

(3) Hung, L. S.; Chen, C. H. *Mater. Sci. Eng. R* **2002**, *39*, 143.

(4) (a) Chen, C. H.; Tang, C. W.; Shi, J.; Klubek, K. P. *Macromol. Symp.* **1997**, *125*, 1. (b) Tang, C. W.; VanSlyke, S. A. *J. Appl. Phys.* **1989**, *65*, 3610. (c) Bulovic, V.; Shoustikov, A.; Baldo, M. A.; Bose, E.; Kozlov, V. G.; Thompson, M. E.; Forrest, S. R. *Chem. Phys. Lett.* **1998**, *287*, 455. (d) Hamada, Y.; Kanno, H.; Tsujioka, T.; Takahashi, H.; Usuki, T. *Appl. Phys. Lett.* **1999**, *75*, 1682. (e) Chen, C. H.; Tang, C. W.; Shi, J.; Klubek, K. P. *Thin Solid Films* **2000**, *363*, 327. (f) Mitsuya, M.; Suzuki, T.; Koyama, T.; Shirai, H.; Taniguchi, Y.; Satsuki, M.; Suga, S. *Appl. Phys. Lett.* **2000**, *77*, 3272. (g) Kim, D. U.; Paik, S. H.; Kim, S.-H.; Tsutsui, T. *Synth. Met.* **2001**, *123*, 43. (h) Zhang, X. H.; Chen, B. J.; Lin, X. Q.; Wong, O. Y.; Lee, C. S.; Kwong, H. L.; Lee, S. T.; Wu, S. K. *Chem. Mater.* **2001**, *13*, 1565. (i) Chen, B.; Lin, X.; Cheng, L.; Lee, C. S.; Gambling, C. W. A.; Lee, S. T. *J. Phys. D: Appl. Phys.* **2001**, *34*, 30. (j) Tao, X. T.; Miyata, S.; Sasabe, H.; Zhang, G. J.; Wada, T.; Jiang, M. H. *Appl. Phys. Lett.* **2001**, *78*, 279. (k) Xie, Z. Y.; Hung, L. S.; Lee, S. T. *Appl. Phys. Lett.* **2001**, *79*, 1048.

(5) (a) Burrows, P. E.; Forrest, S. R.; Sibley, S. P.; Thompson, M. E. *Appl. Phys. Lett.* **1996**, *69*, 2959. (b) Baldo, M. A.; O'Brien, D. F.; You, Y.; Shoustikov, A.; Sibley, S.; Thompson, M. E.; Forrest, S. R. *Nature* **1998**, *395*, 151. (c) O'Brien, D. F.; Baldo, M. A.; Thompson, M. E.; Forrest, S. R. *Appl. Phys. Lett.* **1999**, *74*, 442. (d) Kwong, R. C.; Sibley, S.; Dubovoy, T.; Baldo, M.; Forrest, S. R.; Thompson, M. E. *Chem. Mater.* **1999**, *11*, 3709. (e) Morgado, J.; Cacialli, F.; Iqbal, R.; Moratti, S. C.; Holmes, A. B.; Yahioglu, G.; Milgrom, L. R.; Friend, R. H. *J. Mater. Chem.* **2001**, *11*, 278.

(6) (a) Kido, J.; Nagai, K.; Ohashi, Y. *Chem. Lett.* **1990**, 657. (b) Kido, J.; Nagai, K.; Okuyama, Y.; Skotheim, T. *Chem. Lett.* **1991**, 1267. (c) Kido, J.; Hayase, H.; Hongawa, K.; Nagai, K.; Okuyama, K. *Appl. Phys. Lett.* **1994**, *65*, 2124. (d) McGehee, M. D.; Bergstedt, T.; Zhang, C.; Saab, A. P.; O'Regan, M. B.; Bazan, G. C.; Srdanov, V. I.; Heeger, A. J. *Adv. Mater.* **1999**, *11*, 1349. (e) Adachi, C.; Baldo, M. A.; Forrest, S. R. *J. Appl. Phys.* **2000**, *87*, 8049. (f) Heil, H.; Steiger, J.; Schmechel, R.; von Seggern, H. *J. Appl. Phys.* **2001**, *90*, 5357. (g) Hong, Z.; Liang, C.; Li, R.; Li, W.; Zhao, D.; Fan, D.; Wang, D.; Chu, B.; Zang, F.; Hong, L.-S.; Lee, S. T. *Adv. Mater.* **2001**, *13*, 1241. (h) Sun, P.-P.; Duan, J.-P.; Shih, H.-T.; Cheng, C.-H. *Appl. Phys. Lett.* **2002**, *81*, 792.

(7) (a) Lamansky, S.; Djurovich, P.; Murphy, D.; Abdel-Razzaq, F.; Lee, H.-E.; Adachi, C.; Burrows, P. E.; Forrest, S. R.; Thompson, M. E. *J. Am. Chem. Soc.* **2001**, *123*, 4304. (b) Adachi, C.; Baldo, M. A.; Lamansky, S.; Thompson, M. E.; Kwong, R. C. *Appl. Phys. Lett.* **2001**, *78*, 1622. (c) Lu, W.; Mi, B.-X.; Chan, M. C. W.; Hui, Z.; Zhu, N.; Lee, S.-T.; Che, C.-M. *Chem. Commun.* **2002**, 206. (d) Jiang, X.; Jen, A. K.-Y.; Carlson, B.; Dalton, L. R. *Appl. Phys. Lett.* **2002**, *80*, 713. (e) Duan, J.-P.; Sun, P.-P; Cheng, C.-H. *Adv. Mater.* **2003**, *15*, 224.

(8) (a) Picciolo, L. C.; Murata, H.; Kafafi, Z. H. *Appl. Phys. Lett.* **2001**, *78*, 2378. (b) Picciolo, L. C.; Murata, H.; Kafafi, Z. H. *Proc. SPIE* **2001**, *4105*, 474. (c) Mi, B. X.; Gao, Z. Q.; Liu, M. W.; Chan, K. Y.; Kwong, H. L.; Wong, N. B.; Lee, C. S.; Hung, L. S.; Lee, S. T. *J. Mater. Chem.* **2002**, *12*, 1307.

10.1021/cm034631e CCC: $25.00 
Published on Web 11/14/2003

Amorphous materials which can be deposited as pure thin films should offer an alternate approach for red-emitting devices forthe following reasons: (1) there is no need for cautious control of the dopant's concentration within a very narrow range; (2) careful selection of the host materials for effective energy transfer to the guest, or carrier trapping by the guest can be avoided. So far there are only very limited reports in this aspect. Concentration quenching effect was found to be greatly reduced by the incorporation of sterically congested spacers in the red-emitting molecules 4-(dicyanomethylene)-2-methyl-6-(1,1,7,7-tetramethyljulolidyl- 9-enyl)-4*H*-pyran (DCJT) and 4-(dicyanomethylene)-2-*tert*-butyl-6-(1,1,7,7- tetramethyljulolidyl-9-enyl)-4*H*-pyran (DCJTB).[4a] A sure warrant of red fluorophores to form glassy morphology relies on effective encapsulation of the emitting core. In an earlier report we successfully synthesized amorphous red-emitting materials by encapsulation of the thieno[3,4-*b*]-pyrazine core, the building block of a low band gap polymer, with peripheral diamine.[9] Recently Chen's group also developed dipolar-type amorphous red-emitting materials which could be fabricated into a nondoping device with good performance.[10] In our continual exploration of amorphous red-emitting materials, we initiated another approach: encapsulation of fused aromatic segments. Herein, we report the synthesis of diarylamine-encapsulated benzo[*a*]aceanthrylene compounds, and the results of EL devices fabricated from these new materials.

## Experimental Section

**General Information.** Unless otherwise specified, all the reactions were carried out under a nitrogen atmosphere using standard Schlenk techniques. Solvents were dried by standard procedures. All chromatographic separation was carried out on silica gel (60 M, 230−400 mesh). The $^1$H NMR spectra were recorded on a Bruker AC400 spectrometer. Electronic absorption spectra were measured in dichloromethane using a Cary 50 Probe UV−visible spectrophotometer. Emission spectra were recorded by a Hitachi F-4500 fluorescence spectrometer.

Solution emission quantum yields were measured with reference to Nile Red[11] in dichloromethane according to the method reported by Crosby.[12] Vacuum-deposited thin films (20-nm thickness) of **acen** on transparent quartz substrates were used for the measurement of quantum yields. Similar film of $Alq_3$ was also fabricated for reference. These films were placed at a fixed angle (∼45 °) to both the incident beam and the detector for the emission spectra (excitation wavelength = 400 nm). The quantum yields were estimated from the equation $\Phi_s = \Phi_r(A_r/A_s)(F_s/F_r)(n_s/n_r)^2$ (where $\Phi_s$ is the quantum yield of **acen**; $\Phi_r$ is quantum yield of $Alq_3$; $A_r$ is absorbance of $Alq_3$; $A_s$ is absorbance of **acen**; $F_s$ is integrated area under the emission spectrum of **acen**; $F_r$ is integrated area under the emission spectrum of $Alq_3$; $n_s$ is the refractive index of **acen**; and $n_r$ is the refractive index of $Alq_3$).[13] The $n$ values at $\lambda_{em}$ were measured with MP100-S equipment of Mission Peak Optics, Inc. and the $\Phi_r$ value was taken to be 0.32.[14]

Cyclic voltammetry experiments were performed with a BAS-100 electrochemical analyzer. All measurements were carried out at room temperature with a conventional three-electrode configuration consisting of platinum working and auxiliary electrodes and a nonaqueous $Ag/AgNO_3$ reference electrode. The $E_{1/2}$ values were determined as $^1/_2(E_p^a + E_p^c)$, where $E_p^a$ and $E_p^c$ are the anodic and cathodic peak potentials, respectively. All potentials reported are not corrected for the junction potential. The solvent in all experiments was $CH_2Cl_2$ and the supporting electrolyte was 0.1 M tetrabutylammonium perchlorate. DSC measurements were carried out using a Perkin-Elmer 7 series thermal analyzer at a heating rate of 10 K/min. TGA measurements were performed on a Perkin-Elmer TGA7 thermal analyzer. Mass spectra (EI and MALDI-TOF) were recorded on a JMS-700 double-focusing mass spectrometer and a Viyager DE-PRO mass spectrometer equipped with a nitrogen laser (337 nm), respectively. Elemental analyses were performed on a Perkin-Elmer 2400 CHN analyzer. Only the syntheses of selected compounds are described.

**9,10-Bis-(4-bromo-phenyl)-1-chloro-anthracene (1).** To 1,4-dibromobenzene (10.6 g, 45 mmol) dissolved in diethyl ether (200 mL), 33.75 mL of *n*-butyllithium (1.6 M in hexane) was added slowly at −78 °C. To the suspension 1-chloro-anthraquinone (4.25 g, 17.5 mmol) in ether (150 mL) was added dropwise at −78 °C. The mixture was left to reach room temperature. Cold water (300 mL) was added and the organic phase was separated. The water phase was extracted with ether (3 × 50 mL). The combined organic fractions were dried over magnesium sulfate and the volatiles were removed in vacuo to deliver a foamy residue. To this residue potassium iodide (13.5 g, 81 mmol), sodium hypophosphite monohydrate (16.2 g, 153 mmol), and acetic acid (150 mL) were added, and the mixture was heated under reflux for 4 h. After the mixture cooled the white precipitate was collected, washed with plenty of water, and dried. The compound was used without further purification in subsequent reactions. Yield = 8.60 g (94%). MALDI MS: $m/z$ 519.9 ($M^+$ for $C_{26}H_{15}{}^{79}Br_2{}^{35}Cl$). $^1$H NMR ($CDCl_3$): $\delta$ 7.18 (dd, $J$ = 7.1, 8.8 Hz, 1 H, $C_6H_3$ of anthracene), 7.27 (dd, $J$ = 2.0, 8.5 Hz, 2 H, $C_6H_4$), 7.29 (dd, $J$ = 2.0, 8.1 Hz, 2 H, $C_6H_4$), 7.31−7.37 (m, 2 H, $C_6H_4$ of anthracene), 7.48 (dd, $J$ = 1.2, 7.1 Hz, 1 H, $C_6H_3$ of anthracene), 7.52−7.59 (m, 3 H, $C_6H_3$, $C_6H_4$ of anthracene), 7.62 (dd, $J$ = 2.0, 8.1 Hz, 2 H, $C_6H_4$), 7.73 (dd, $J$ = 2.0, 8.5 Hz, 2 H, $C_6H_4$). Anal. Calcd for $C_{26}H_{15}Br_2Cl$: C, 59.75; H, 2.89. Found: C, 59.39; H, 2.85.

**General Procedures for the Cyclization of Benzo[*a*]-aceanthrylene.** Compounds 8-(4-diphenylamino-phenyl)- benzo[*a*]aceanthrylen-3-yl]-diphenyl-amine (**2**), [4-(3-carbazol-9-yl- benzo[*a*]aceanthrylen-8-yl)-phenyl]-carbazole (**3**), naphthalen-1-yl-{8-[4- (naphthalen-1-yl-phenyl-amino)-phenyl]- benzo-[*a*]aceanthrylen-3-yl}-phenyl-amine (**4**), (4-*tert*-butyl-phenyl)-(8-{4-[(4-*tert*-butyl-phenyl)-(4-ethyl-phenyl)-amino]- phenyl}-benzo[*a*]aceanthrylen-3-yl)-(4-ethyl-phenyl)-amine (**5**), and anthracen-9-yl- (8-{4-[anthracen-9-yl-(4-ethyl-phenyl)-amino]-phenyl}-benzo[*a*]-aceanthrylen-3-yl)-(4-ethyl-phenyl)-amine (**6**) were synthesized by a procedure similar to that described in the next paragraph. The corresponding amino intermediates are commercially available except for (4-*tert*-butyl-phenyl)-(4-ethyl-phenyl)-amine (**5a**) and anthracen-9-yl-(4-ethyl-phenyl)-amine (**6a**). These two compounds were obtained with satisfactory elemental analyses from $Pd(OAc)_2$/*t*-BuONa/tris(*tert*-butyl)phosphine catalyzed coupling reactions of 4-ethyl-phenylamines with 1-bromo-4-*tert*-butyl-benzene and 9-bromo-anthracene, respectively.

A two-necked flask was charged with $Pd(OAc)_2$ (0.01 mol % per bromo atom), *t*-BuONa (1.2 equiv. per bromo atom), bromides (1.0 mmol), and amines (1 equiv per bromo atom). Dry toluene was added and the reaction mixture was stirred under nitrogen for 20 min. Tris(*tert*-butyl)phosphine (0.02 mol %) in dry toluene was added through a syringe (the stock solution contained 0.88 mmol of phosphine in 1 mL of dry toluene). The reaction mixture was heated under reflux until amine was consumed. After cooling, the mixture was extracted with water and ether. The organic phase was dried over anhydrous $MgSO_4$ and then the volatile was removed. A one-necked flask was charged with the residue and KOH (2 equiv per chloro atom). Quinoline was added, and the reaction was

(9) Justin Thomas, K. R.; Lin, J. T.; Tao, Y.-T.; Chuen, C.-H. *Adv. Mater.* **2002**, *14*, 822.
(10) Wu, W.-C.; Yeh, H.-C.; Chan, L.-H.; Chen, C.-T. *Adv. Mater.* **2002**, *14*, 1072.
(11) Sarkar, N.; Das, K.; Nath, D. N.; Bhattacharyya, K. *Langmuir* **1994**, *10*, 326.
(12) Demas, J. N.; Crosby, G. A. *J. Phys. Chem.* **1971**, *75*, 991.
(13) Demas, J. N.; Crosby, G. A. *J. Phys. Chem.* **1971**, *75*, 991.
(14) Garbuzov, D. Z.; Bulovic, V.; Burrows, P. E.; Forrest, S. R. *Chem. Phys. Lett.* **1996**, *249*, 433.

stirred and heated under reflux for 6 h. After cooling, the mixture was diluted with ether and the organic phase was washed with HCl solution (concentrated: 10%, 3 × 50 mL). After this mixture was dried over $MgSO_4$ and the volatile was removed, the residue was purified by column chromatography using hexanes and $CH_2Cl_2$ as eluant.

**Compound 2.** Red solid. Yield = 1.20 g (35%). MALDI MS: *m/z* 662 ($M^+$). $^1$H NMR ($CDCl_3$): $\delta$ 7.02−7.06 (m, 4 H, *para*-$C_6H_5$), 7.20−7.38 (m, 21 H, *ortho*-$C_6H_5$, *meta*-$C_6H_5$, $C_6H_4$), 7.44 (dd, $J$ = 6.5, 8.8 Hz, 1 H, $C_6H_4$ of anthracene), 7.49 (dd, $J$ = 6.5, 8.6 Hz, 1 H, $C_6H_3$ of anthracene), 7.57 (dd, $J$ = 6.5, 8.7 Hz, 1 H, $C_6H_4$ of anthracene), 7.74 (s, 1 H, $C_6H_3$), 7.76 (d, $J$ = 8.6 Hz, 1 H, $C_6H_3$ of anthracene), 7.82 (d, $J$ = 6.5 Hz, 1 H, $C_6H_3$ of anthracene), 8.04 (d, $J$ = 8.8 Hz, 1 H, $C_6H_4$ of anthracene), 8.22 (d, $J$ = 8.4 Hz, 1 H, $C_6H_3$), 8.70 (d, $J$ = 8.7 Hz, 1 H, $C_6H_4$ of anthracene). Anal. Calcd for $C_{50}H_{34}N_2$: C, 90.60; H, 5.17; N, 4.22. Found: C, 90.77; H, 5.15; N, 4.00.

**Compound 3.** Red solid. Yield = 980 mg (30%). MALDI MS: *m/z* 658 ($M^+$). $^1$H NMR ($CDCl_3$): $\delta$ 7.31−7.37 (m, 4 H, $C_6H_4$ of carbazole), 7.44−7.53 (m, 4 H, $C_6H_4$ of carbazole), 7.55−7.59 (m, 3 H, $C_6H_4$ of anthracene, $C_6H_4$ of carbazole), 7.65−7.69 (m, 3 H, $C_6H_3$ of anthracene, $C_6H_4$ of carbazole), 7.71 (dd, $J$ = 2.0, 8.1 Hz, 1 H, $C_6H_3$), 7.76−7.77 (m, 1 H, $C_6H_4$ of anthracene), 7.79 (dd, $J$ = 2.1, 8.5 Hz, 2 H, $C_6H_4$), 7.84 (dd, $J$ = 2.1, 8.5 Hz, 2 H, $C_6H_4$), 7.89 (dd, $J$ = 0.3, 8.1 Hz, 1 H, $C_6H_3$), 8.07 (d, $J$ = 6.6 Hz, 1 H, $C_6H_4$ of anthracene), 8.14 (d, $J$ = 8.6 Hz, 1 H, $C_6H_4$ of anthracene), 8.19−8.22 (m, 4 H, $C_6H_4$ of carbazole), 8.22 (d, $J$ = 2.0 Hz, 1 H, $C_6H_3$), 8.66 (d, $J$ = 8.1 Hz, 1 H, $C_6H_3$ of anthracene), 8.94 (d, $J$ = 8.7 Hz, 1 H, $C_6H_4$ of anthracene). Anal. Calcd for $C_{50}H_{30}N_2$: C, 91.16; H, 4.59; N, 4.25. Found: C, 91.15; H, 4.52; N, 4.02.

**Compound 4.** Red solid. Yield = 1.30 g (62%). MALDI MS: *m/z* 762 ($M^+$). $^1$H NMR ($CDCl_3$): $\delta$ 6.96−7.00 (m, 2 H, *para*-$C_6H_5$), 7.09 (d, $J$ = 4.2 Hz, 1 H, $C_6H_3$ of anthracene), 7.13 (d, $J$ = 7.9 Hz, 2 H, *ortho*-$C_6H_5$), 7.18 (m, 21 H, *ortho*-$C_6H_5$, *meta*-$C_6H_5$, $C_6H_4$, $C_6H_3$, $C_6H_3$ of naphthalene, $C_6H_4$ of naphthalene, $C_6H_4$ of anthracene), 7.73−7.75 (m, 2 H, $C_6H_4$ of naphthalene), 7.79−7.83 (m, 3 H, $C_6H_3$, $C_6H_4$ of naphthalene), 7.90 (d, $J$ = 7.9 Hz, 1 H, $C_6H_4$ of naphthalene), 7.91 (d, $J$ = 7.9 Hz, 1 H, $C_6H_4$ of naphthalene), 8.02−8.06 (m, 2 H, $C_6H_4$ of anthracene, $C_6H_4$ of naphthalene), 8.09 (d, $J$ = 8.2 Hz, 1 H, $C_6H_3$), 8.17 (d, $J$ = 8.5 Hz, 1 H, $C_6H_3$ of anthracene), 8.67 (d, $J$ = 8.5 Hz, 1 H, $C_6H_4$ of anthracene). Anal. Calcd for $C_{58}H_{38}N_2$: C, 91.31; H, 5.02; N, 3.67. Found: C, 91.38; H, 5.34; N, 3.33.

**Compound 5.** Red solid. Yield = 1.02 g (54%). MALDI MS: *m/z* 831 ($M^+$). $^1$H NMR ($CDCl_3$): $\delta$ 1.26 (t, $J$ = 7.5 Hz, 6 H, $CH_3$), 1.33 (s, 18 H, $CH_3$), 2.64 (q, $J$ = 7.5 Hz, 4 H, $CH_2$), 7.00−7.30 (m, 21 H, $C_6H_4$, $C_6H_3$), 7.41 (t, $J$ = 7.2 Hz, 1 H, $C_6H_4$ of anthracene), 7.52 (t, $J$ = 8.1 Hz, 1 H, $C_6H_3$ of anthracene), 7.60 (t, 1 H, $C_6H_4$ of anthracene), 7.74 (s, 1 H, $C_6H_3$), 7.79 (d, $J$ = 8.6 Hz, 1 H, $C_6H_3$ of anthracene), 7.85 (d, $J$ = 6.5 Hz, 1 H, $C_6H_3$ of anthracene), 8.07 (d, $J$ = 8.7 Hz, 1 H, $C_6H_4$ of anthracene), 8.21 (d, $J$ = 8.4 Hz, 1 H, $C_6H_3$), 8.71 (d, $J$ = 8.7 Hz, 1 H, $C_6H_4$ of anthracene). Anal. Calcd for $C_{62}H_{58}N_2$: C, 89.60; H, 7.03; N, 3.37. Found: C, 89.38; H, 6.88; N, 3.13.

**Compound 6.** Red solid. Yield = 230 mg (12%). MALDI MS: *m/z* 919 ($M^+$). $^1$H NMR ($CDCl_3$): $\delta$ 1.17−1.26 (m, 6 H, $CH_3$), 2.53−2.59 (m, 4 H, $CH_2$), 6.99−7.05 (m, 5 H, $C_6H_4$), 7.11−7.13 (m, 2 H, $C_6H_5$), 7.16−7.18 (m, 4 H, $C_6H_4$), 7.23−7.24 (m, 2 H, $C_6H_3$, $C_6H_4$ of anthracene), 7.32−7.53 (m, 11 H, $C_6H_4$, $C_6H_4$ of anthracene, $C_6H_3$ of anthracene), 7.69 (d, $J$ = 8.6 Hz, 1 H, $C_6H_4$ of anthracene), 7.73 (d, $J$ = 6.6 Hz, 1 H, $C_6H_3$ of anthracene), 7.80 (s, 1 H, $C_6H_3$), 7.98 (d, $J$ = 8.6 Hz, 1 H, $C_6H_4$ of anthracene), 8.06−8.09 (m, 5 H, $C_6H_3$, $C_6H_4$ of anthracene), 8.21−8.28 (m, 4 H, $C_6H_4$ of anthracene), 8.52 (s, 2 H, $C_6H$ of anthracene), 8.59 (d, $J$ = 8.6 Hz, 1 H, $C_6H_4$ of anthracene). Anal. Calcd for $C_{70}H_{50}N_2$: C, 91.47; H, 5.48; N, 3.05. Found: C, 91.33; H, 5.59; N, 3.03.

**LEDs Fabrication and Measurement.** Electron-transporting materials TPBI (1,3,5-tris(*N*-phenylbezimidazol-2-yl)-benzene) and $Alq_3$ (tris(8-hydroxyquinoline) aluminum) were synthesized according to literature procedures,[15] and were sublimed twice prior to use. Prepatterned ITO substrates with an effective individual device area of 3.14 $mm^2$ were cleaned as described in a previous report.[16] Double-layer EL devices using **2**−**6** as the hole-transport and emitting layer and TPBI or $Alq_3$ as the electron-transport layer were fabricated. All devices were prepared by vacuum deposition of 40 nm of the hole-transporting layer, followed by 40 nm of TPBI or $Alq_3$. An alloy of magnesium and silver (ca. 10:1, 50 nm) was deposited as the cathode, which was capped with 100 nm of silver. I−V curves were measured on a Keithley 2400 Source Meter in ambient environment. Light intensity was measured with a Newport 1835 Optical Meter.

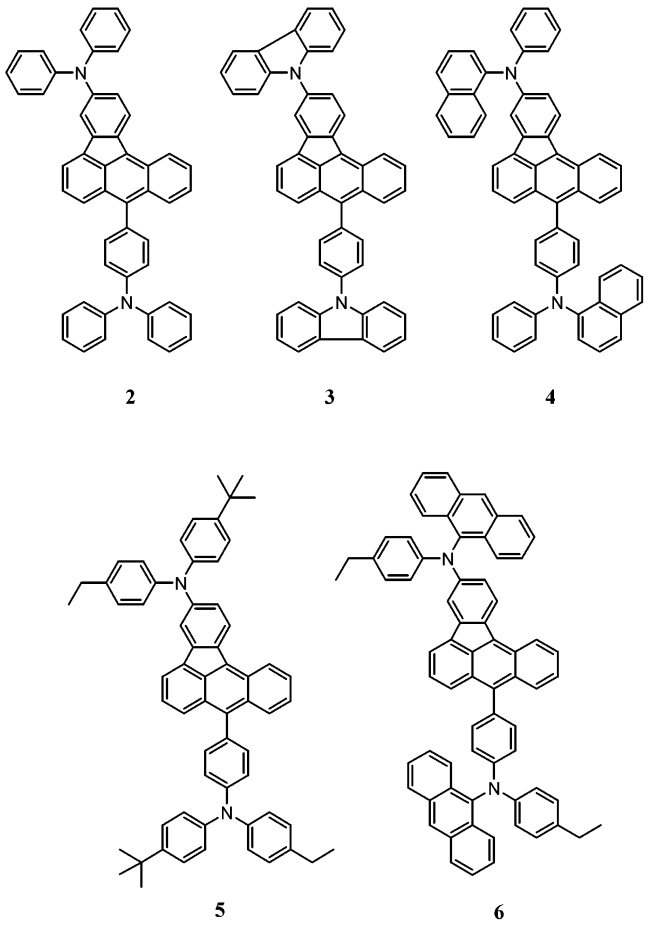


**Figure 1.** Structures of the **acen** compounds.

## Results and Discussion

**Synthesis of the Compounds and Thermal Properties.** The new compounds synthesized in this study are illustrated in Figure 1. Scheme 1 outlines the synthetic sequence for the new compounds. There are three key steps: (1) conversion of 1-chloro-anthraquinone to 1-chloro-9,10-disubstituted anthracene **1** by using the method reported by Dehaen[17] and us;[18] (2) palladium catalyzed aromatic C−N coupling reactions developed by Koie[19] and Hartwig;[20] and (3) cyclization

(15) (a) Sonsale, A. Y.; Gopinathan, S.; Gopinathan, C. *Indian J. Chem.* **1976**, *14*, 408. (b) Shi, J.; Tang, C. W.; Chen, C. H. U.S. Patent 5,645,948, 1997. (C) Chen, C. H.; Shi, J.; Tang, C. W. *Coord. Chem. Rev.* **1998**, *171*, 161.

(16) Balasubramaniam, E.; Tao, Y. T.; Danel, A.; Tomasik, P. *Chem. Mater.* **2000**, *12*, 2788.

(17) Smet, M.; Shukla, R.; Fülöp, L.; Dehaen, W. *Eur. J. Org. Chem.* **1998**, *2769*.

(18) Danel, K.; Huang, T.-H.; Lin, J. T.; Tao, Y.-T.; Chuen, C.-H. *Chem. Mater.* **2002**, *14*, 3860.

(19) Yamamoto, T.; Nishiyama, M.; Koie, Y. *Tetrahedron Lett.* **1998**, *39*, 2367.

**Table 1. Absorption, Emission, and Electrochemical Data of the Red Dyes**

| parameter/ compd | 2 | 3 | 4 | 5 | 6 |
|---|---|---|---|---|---|
| $T_g/T_m/T_d$ | 113/224/430 | 178/299/460 | 151/393/420 | 143/na[e]/440 | 202/na/440 |
| $\lambda_{max}$, nm in toluene | 510, 438, 414, 352 | 460, 331 | 510, 435, 413, 349 | 520, 439, 359 | 552 (sh), 520, 440, 325 |
| $\lambda_{em}$, nm ($\Phi_f$, %) in toluene[a] | 615 (8) | 558 (35) | 611 (11) | 623 (10) | 610 (12) |
| $\lambda_{em}$, nm ($\Phi_f$, %) in $CH_2Cl_2$[a] | 638 (5) | 572 (23) | 636 (7) | 661 (5) | 634 (9) |
| $\lambda_{em}$, nm in pyridine | 643 | 573 | 636 | 659 | 652 |
| $\lambda_{em}$, nm ($\Phi_f$, %) film[b] | 627 (4) | 575 (sh), 610 (16) | 623 (9) | 637 (9) | 636 (4), 715 (sh) |
| $E$ ($\Delta E_p$), mV[c] | 382 (120), 555 (112), −848(201) | 583 (122), −783 (285) | 341 (110), 529 (115), −905 (174) | 384 (114), 573 (112), −1020 (105) | 288 (91), 494 (98), −773 (65) |
| HOMO/LUMO, eV[d] | 5.18/3.15 | 5.38/3.12 | 5.13/3.06 | 5.18/3.29 | 5.09/3.12 |

[a] Quantum yield was measured relative to Nile Red in $CH_2Cl_2$. Corrections due to the change in solvent refractive indices were applied. [b] Thin films (20-nm thickness) of **acen** were deposited on transparent quartz substrates for the measurements. The quantum yields were estimated by using the equation, $\Phi_s = \Phi_r(A_r/A_s)(F_s/F_r)(n_s/n_r)^2$, where *s* and *r* are **acen** and $Alq_3$, respectively (see Experimental Section).[13] [c] Measured in $CH_2Cl_2$. All the potentials are reported relative to ferrocene which was used as internal standard in each experiment. Ferrocene oxidation potential was located at +517 mV ($\Delta E_p$ = 108 mV) relative to $Ag/AgNO_3$ nonaqueous reference electrode. The concentration of the compound was $2.5 \times 10^{-4}$ M and the scan rate was 100 mV/s. [d] HOMO energy was calculated with reference to ferrocene (4.8 eV). Solvent to vacuum correction was not applied. Band gap was derived from the observed optical edge and LUMO energy was derived from the relation band gap = HOMO − LUMO. [e] na: not observed.

**Scheme 1**

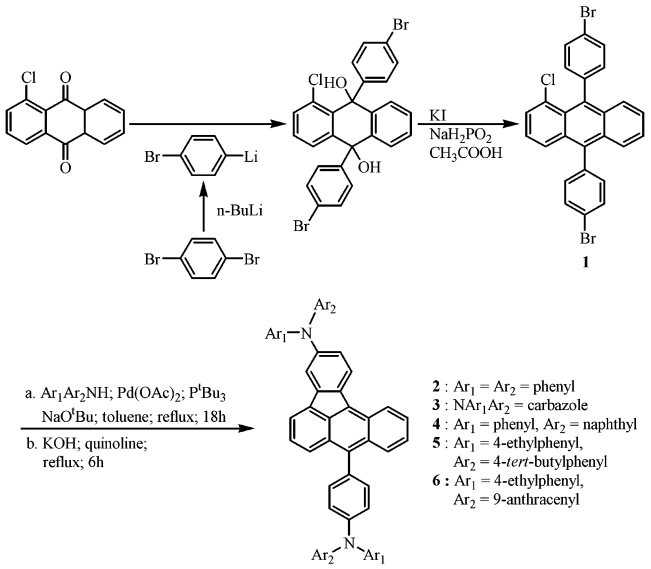


of the diphenylanthracene to form benzo[*a*]aceanthrylene derivatives **2**−**6** (**acen**) according to the Dehaen's method.[17] Steps 2 and 3 were carried out sequentially without isolation of the intermediates.

The thermal properties of the new compounds were determined by DSC and TGA measurements (Table 1). The compounds are amorphous once made (**5** and **6**) or readily form a glass (**2**, **3**, and **4**) upon cooling (10 K/min) of the melt and the glassy state persists in the subsequent heating cycles as shown by DSC measurements. Obviously, diarylamine segments help to suppress the aggregation of the flat benzo[*a*]aceanthrylene core. The incorporation of *tert*-butyl groups in the phenyl ring results in an increase of the $T_g$s (**2** vs **5**), which is in accordance with a literature report.[21] Very high $T_g$

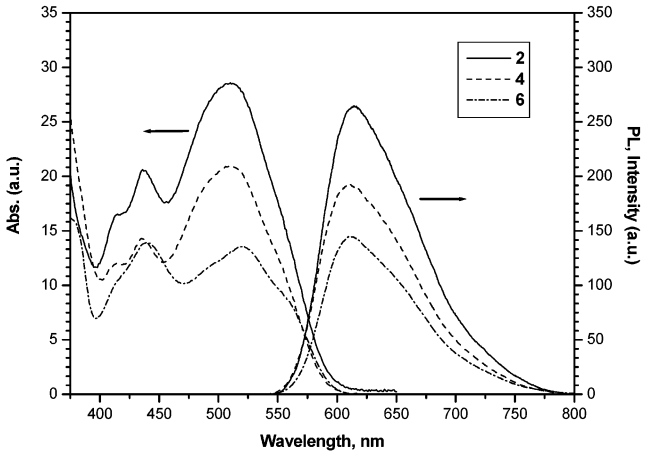


**Figure 2.** Absorption and emission spectra of compounds **2**, **4**, and **6**.

materials were obtained upon incorporation of rigid carbazolyl (**3**, $T_g$ = 178 °C) or anthracenyl (**6**, $T_g$ = 202 °C) segments.[22] The high glass transition temperatures ($T_g$ = 113−202 °C) and thermal decomposition temperatures ($T_d$ = 420−460 °C) of the compounds (Table 1) should be beneficial to the stability of the deposited films.

**Optical Properties.** The absorption and luminescence data of the compounds are presented in Table 1. Representative absorption and emission spectra are shown in Figure 2. These compounds have a prominent $\pi-\pi^*$ transition band appearing at $\lambda_{max} \approx 460-520$ nm (in toluene) in the electronic absorption spectra, and exhibit a moderate Stokes shift in the emission spectra ($\Delta\lambda_{em} \approx 90-113$ nm in toluene). The relatively small Stokes shift of the fluorescence spectra may result in partial bleaching of emission and lower the quantum yield of **acen**. Except for compound **3** which emits

(20) Hartwig, J. F.; Kawatsura, M.; Hauck, S. I.; Shaughnessy, L. M.; Alcazar-Roman, J. *J. Org. Chem.* **1999**, *64*, 5575.
(21) Jandke, M.; Strohriegl, P.; Berleb, S.; Werner, E.; Brutting, W. *Macromolecules* **1998**, *31*, 6434.
(22) (a) Thelakkat, M.; Schmitz, C.; Hohle, C.; Strohriegl, P.; Schmidt, H.-W.; Hofmann, U.; Schloter, S.; Haarer, D. *Phys. Chem. Chem. Phys.* **1999**, *1*, 1693. (b) Steuber, F.; Staudigel, J.; Stossel, M.; Simmerer, J.; Winnacker, A.; Spreitzer, H.; Weissortel, F.; Salbeck, J. *Adv. Mater.* **2000**, *12*, 130. (c) Shirota, Y. *J. Mater. Chem.* **2000**, *10*, 1.

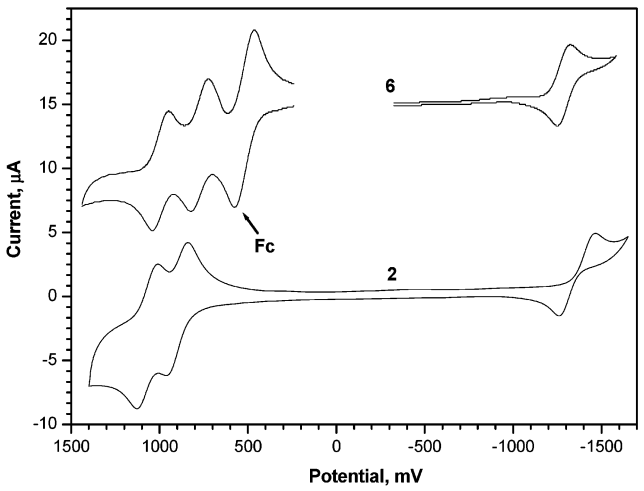


**Figure 3.** Cyclic voltammograms of **2** and **6** in deoxygenated $CH_2Cl_2$ containing 0.1 M TBAP at 25 °C. Ferrocene was added to the solution of compound **6** as an internal standard. All potentials are in volts vs $Ag/AgNO_3$ (0.01 M in MeCN; the scan rate is 80 $mVs^{-1}$).

yellow-orange light ($\lambda_{em} = 572$ nm in dichloromethane), all other compounds emit in the red region ($\lambda_{em} \approx 634-661$ nm in dichloromethane). Proper electron-donating substituents at the 5- and/or 12-position of the rubicene moiety were found to bathochromically shift the $\lambda_{em}$ to the red region.[17] Similarly, incorporation of the diarylamine moiety helps to tune the $\lambda_{em}$ of the benzo[*a*]aceanthrylene compounds to the red. The emission likely originated from $\pi \rightarrow \pi^*$ excited state mixed with some $n \rightarrow \pi^*$ character based on the following observations: (a) the emission wavelength exhibits a moderate positive solvatochromism (i.e., $\lambda_{em}$ (toluene) < $\lambda_{em}$ (pyridine)); (b) the $\lambda_{em}$ is found to increase (**3** < **2** < **5**) in accordance with the electron-donating ability of the arylamines. Rigidity of the carbazolyl moiety will hamper its conjugation with the aryl segment at the nitrogen atom in triarylamines.[23] Therefore, it is common that the carbazolyl derivative exhibits shorter $\lambda_{max}$ and $\lambda_{em}$ among triarylamine homologues.[24] It is interesting to note that compound **3** has a significantly higher fluorescence quantum yield than others; possibly the rigidity of the carbazolyl moiety prevents the free rotation of the C−N bond which may deactivate the excited-state nonradiatively. It is also possible that there is less tendency for reductive quenching to occur because of the higher oxidation potential of the carbazolyl nitrogen than that of the diphenylamine nitrogen.

**Electrochemical Properties.** Electrochemical characteristics of the new compounds were investigated by using cyclic voltammetric methods, and the redox properties of the new compounds are collected in Table 1. Representative cyclic voltammograms are shown in Figure 3. Each compound except **3** displays two quasi-reversible waves at relatively low oxidation potentials attributable to the successive oxidation of two different arylamine units. The amine whose nitrogen atom is linked to the benzo[*a*]aceanthrylene core is expected to be oxidized at a lower potential than the other because the benzo[*a*]aceanthrylene has higher electron density than the phenyl ring. In accordance with the observation of Thompson,[24a] compound **3** exhibits a significantly higher oxidation potential because of the presence of the carbazole unit. A quasi-reversible reduction wave attributable to the reduction of the benzo[*a*]aceanthrylene core is also observed in all of the compounds.

**Electroluminescent Properties.** The HOMO energy levels of **acen** were calculated from cyclic voltammetry (vide supra) and by comparison with ferrocene (4.8 eV).[25] These together with absorption spectra were then used to obtain the LUMO energy levels (Table 1).[24a,26]

Two types of double-layer devices using **2**−**6** (**acen**) as both hole-transport and emitting materials, and TPBI (1,3,5-tris(*N*-phenylbenzimidazol-2-yl)benzene) or $Alq_3$ (tris(8-hydroxyquinoline)aluminum) as the electron-transport materials, were fabricated (Figure 4): (I) ITO/**acen** (40 nm)/TPBI (40 nm)/Mg:Ag; (II) ITO/**acen** (40 nm)/$Alq_3$ (40 nm)/Mg:Ag. The current−voltage−luminance ($I-V-L$) characteristics are shown in Figures 5 and 6. Figure 7 shows the EL spectra of the devices I and II. The EL spectra of the devices I (Figure 7a) are the same as the PL spectra of **acen**, except that minor emission around 380 nm attributed to TPBI was observed.[27] On the basis of the energy level diagram (Figure 8), the smaller HOMO energy gap between **3** and TPBI should result in more leakage of the holes to TPBI. Consequently, more TPBI emission was detected. The device I of **2**, **4**, and **6** have pure red emission with CIE coordinates (Table 2) comparable to that of the National Television System Committee (NTSC) standard red color ($x = 0.64$, $y = 0.32$). Emission also mainly came from **acen** in the devices II (Figure 7b), however, significant contribution from $Alq_3$ was detected and the CIE coordinates fall in the yellow-orange region. Analysis of the energy level diagram (Figure 8) suggests that the passage of the holes from **acen** to the ETL is more

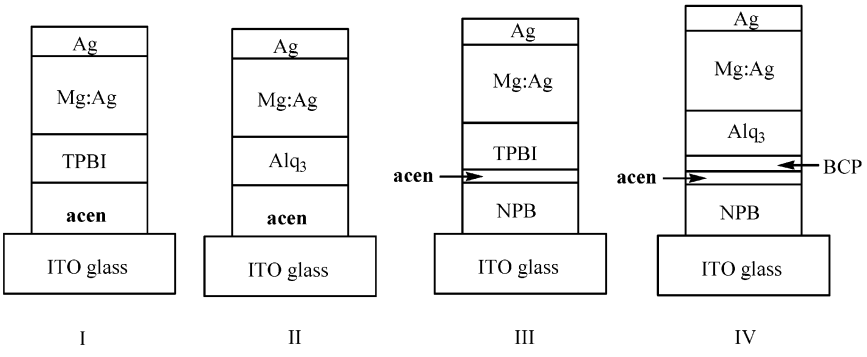


**Figure 4.** Schematic diagram of EL device configurations. I: ITO/**acen** (40 nm)/TPBI (40 nm)/Mg:Ag/Ag. II: ITO/**acen** (40 nm)/$Alq_3$ (40 nm)/Mg:Ag/Ag. III: ITO/NPB (40 nm)/**acen** (10 nm)/TPBI (40 nm)/Mg:Ag/Ag. IV: ITO/NPB (40 nm)/**acen** (10 nm)/BCP (10 nm)/$Alq_3$ (40 nm)/Mg:Ag/Ag.

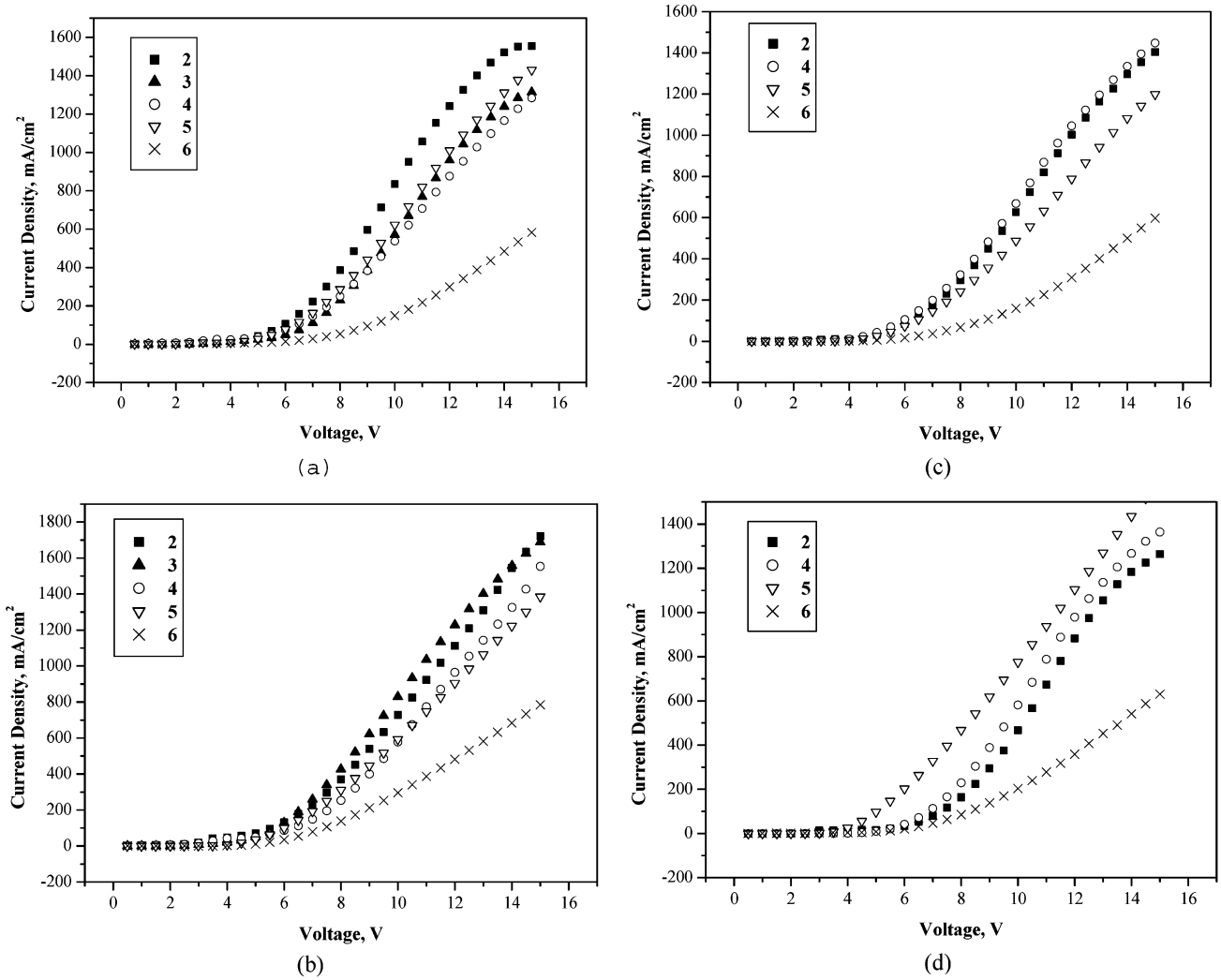


**Figure 5.** Current density vs applied electric field characteristics of the devices I (a), II (b), III (c), and IV (d).

effectively blocked in the device I than in II due to the lower HOMO level of TPBI (6.20 eV) than $Alq_3$ (6.00 eV). The superior hole-transporting than electron-transporting ability of **acen** may also be the cause of $Alq_3$ emission in the devices II. The better performance for both devices fabricated from **3** may be attributed to the significantly higher solution quantum yield of **3** compared to that of the other compounds. An unusual feature of the compound **6** is the appearance of a shoulder at $\lambda \approx 715$ nm in the EL spectra of both the devices I and II. This characteristic peak was also observed in the PL spectra of the deposited film of **6**. We tentatively attribute this to excimer instead of exciplex emission. Exciplex formation is unlikely based on the following observations: (1) no such peak was observed in PL spectra of deposited films TPBI/**6** (98:2) and $Alq_3$/**6** (98:2), and devices using **6** as dopant, ITO/NPB (40 nm)/TPBI (40 nm)/2% **6**/Mg:Ag and ITO/NPB (40 nm)/$Alq_3$ (30 nm)/2% **6**/Mg:Ag (NPB = 4,4′-bis[(1-naphthylphenyl)amino]biphenyl). It is interesting to note that the intensity of the shoulder in PL increases as the film thickness of **6** increases. In the devices III and IV (vide infra) which have a thinner film of **6** (10 nm), there was no shoulder detectable either.

Two other devices were also fabricated where red-emitting **acen** (**2**, **4**, **5**, and **6**) were used as the emission layer: (III) ITO/NPB (40 nm)/**acen** (10 nm)/TPBI (40 nm)/Mg:Ag; (IV) ITO/NPB (40 nm)/**acen** (10 nm)/BCP (10 nm)/$Alq_3$ (30 nm)/Mg:Ag (NPB = 4,4′-bis[(1-naphthylphenyl)amino]biphenyl), HOMO = 5.2 eV, LUMO = 2.2 eV;[27] BCP = bathocuproine, HOMO = 6.4 eV, LUMO = 2.9 eV[28]). The current−voltage−luminance ($I-V-L$) characteristics are shown in Figures 5 and 6, and the EL spectra are shown in Figure 7. These devices show a performance close to that of the devices of type I. Similar to the device I, there is no significant variation of performance vs the drive voltage. Importantly, both devices have pure red emission from **acen** though very minor emission from TPBI was still observed in the device III. Both devices I and III of compound **5** have the most TPBI contribution among compounds **2** and

(23) Yang, J.-S.; Chiou, S.-Y.; Liau, K.-L. *J. Am. Chem. Soc.* **2002**, *124*, 2518.
(24) (a) Koene, B. E.; Loy, D. E.; Thompson, M. E. *Chem. Mater.* **1998**, *10*, 2235. (b) Wu, I.-Y.; Lin, J. T.; Tao, Y.-T.; Balasubramaniam, E. *Adv. Mater.* **2000**, *12*, 668. (c) Wu, I.-Y.; Lin, J. T.; Tao, Y.-T.; Balasubramaniam, E.; Su, Y. Z.; Ko, C.-W. *Chem. Mater.* **2001**, *13*, 2626.
(25) Pommerehne, J.; Vestweber, H.; Guss, W.; Mahrt, R. F.; Bässler, H.; Porsch, M.; Daub, J. *Adv. Mater.* **1995**, *7*, 551.
(26) Thelakkat, M.; Schmidt, H.-W. *Adv. Mater.* **1998**, *10*, 219.
(27) Tao, Y.-T.; Balasubramaniam, E.; Danel, A.; Tomasik, P. *Appl. Phys. Lett.* **2000**, *77*, 933.
(28) Baldo, M. A.; Thompson, M. E.; Forrest, S. R. *Pure Appl. Chem.* **1999**, *71*, 2095.

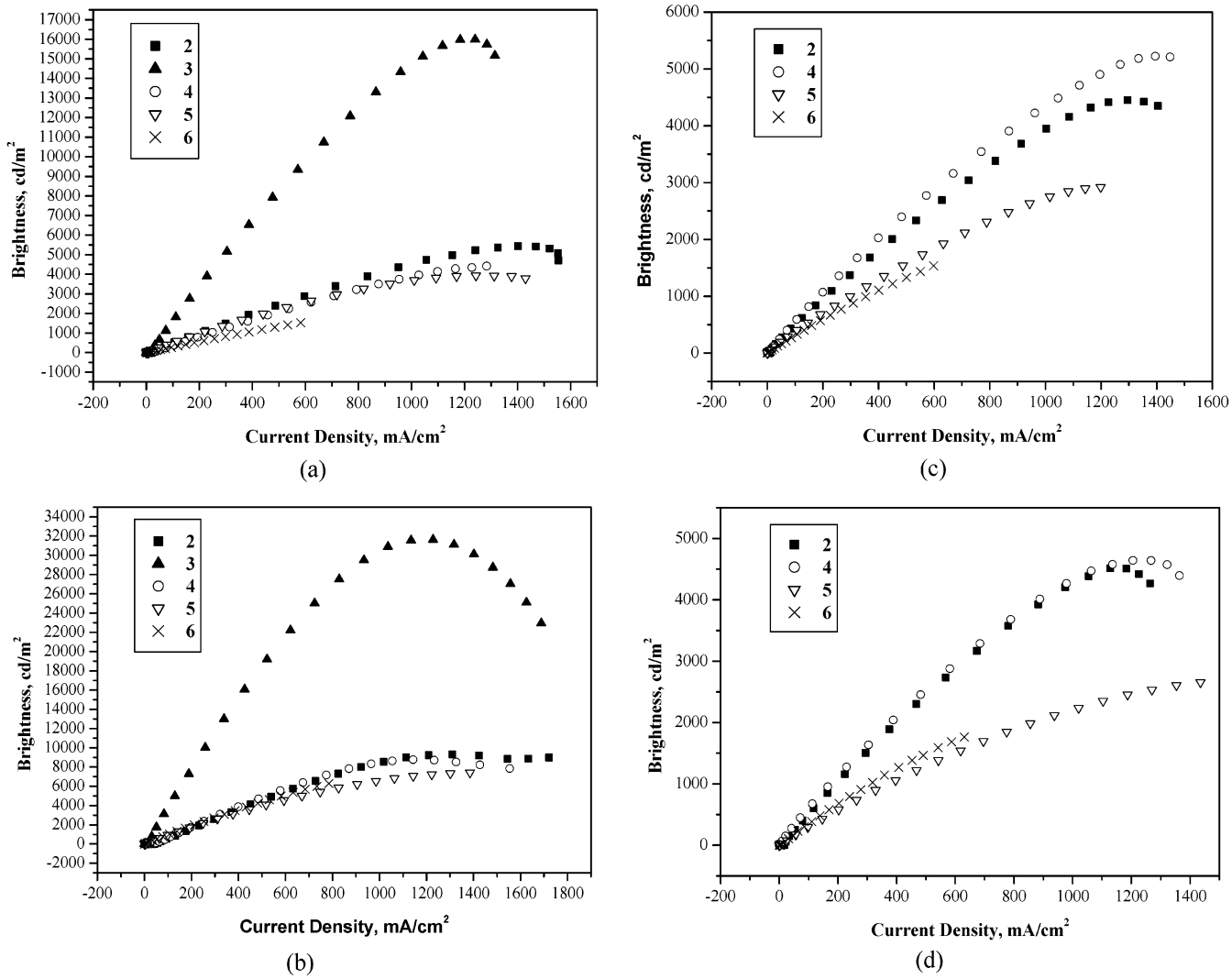


**Figure 6.** Luminance versus current density characteristics of the devices I (a), II (b), III (c), and IV (d).

**Table 2. Electroluminescent Data of the Devices**[a]

| | 2 | 3 | 4 | 5 | 6 |
|---|---|---|---|---|---|
| $V_{on}$, V | 3.4; 3.6; 3.4; 4.2 | 4.1; 3.4 | 3.8; 3.8; 3.3; 3.8 | 3.8; 3.5; 3.7; 4.1 | 3.9; 3.6; 3.4; 4.0 |
| $L_{max}$, cd/m² | 5436 (13); 9315 (13); | 15993 (14); | 4416 (15); 8765 (13); | 3936 (14); 7432 (15); | 1528 (15); 6279 (15); |
| ($V$ at $L_{max}$, V) | 4451 (14); 4514 (14) | 31632 (12) | 5225 (15); 4643 (14) | 2921 (15); 2705 (15) | 1534 (15); 1764 (15) |
| $\lambda_{em}$, nm | 624; 624; 624; 626 | 578; 566 | 624; 622; 622; 624 | 632; 630; 630; 632 | 630; 624; 628; 626 |
| CIE ($x$,$y$) | 0.64, 0.34; 0.51, 0.43; | 0.51, 0.45; | 0.64, 0.34; 0.53, 0.42; | 0.62, 0.31; 0.49, 0.43; | 0.64, 0.32; 0.45, 0.46; |
| | 0.63, 0.34; 0.65, 0.35 | 0.46, 0.49 | 0.64, 0.34; 0.65, 0.35 | 0.59; 0.30; 0.65, 0.34 | 0.64, 0.33; 0.66, 0.34 |
| $\eta_{ext,max}$, % | 0.46; 0.58; 0.48; 0.49 | 0.73; 1.40 | 0.39; 0.63; 0.51; 0.68 | 0.63; 0.68; 0.49; 0.33 | 0.40; 0.64; 0.36; 0.37 |
| $\eta_{p,max}$, lm/W | 0.26; 0.37; 0.33; 0.23 | 0.74; 2.2 | 0.18; 0.37; 0.38; 0.60 | 0.30; 0.74; 0.33; 0.27 | 0.12; 0.66; 0.30; 0.17 |
| $\eta_{c,max}$, cd/A | 0.50; 0.91; 0.53; 0.52 | 1.7; 3.9 | 0.42; 0.97; 0.57; 0.77 | 0.53; 0.99; 0.42; 0.31 | 0.28; 1.02; 0.33; 0.36 |
| $L$, cd/m² (at 100 mA/cm²) | 492; 577; 503; 516 | 1601; 3796 | 360; 623; 561; 604 | 512; 940; 383; 299 | 283; 967; 309; 350 |
| $\eta_{ext}$, % (at 100 mA/cm²) | 0.44; 0.36; 0.46; 0.48 | 0.68; 1.41 | 0.33; 0.40; 0.50; 0.54 | 0.61; 0.64; 0.43; 0.32 | 0.40; 0.61; 0.33; 0.37 |
| $\eta_p$, lm/W (at 100 mA/cm²) | 0.26; 0.32; 0.26; 0.22 | 0.73; 2.1 | 0.18; 0.31; 0.30; 0.28 | 0.26; 0.49; 0.19; 0.27 | 0.10; 0.41; 0.11; 0.13 |
| $\eta_c$, cd/A (at 100 mA/cm²) | 0.49; 0.57; 0.51; 0.52 | 1.6; 3.8 | 0.36; 0.61; 0.56; 0.61 | 0.51; 0.94; 0.38; 0.31 | 0.28; 1.04; 0.97; 0.30 |

[a] The measured values are given in order of the devices I, II, III, and IV. $L_{max}$, maximum luminance; $L$, luminance; $V_{on}$, turn-on voltage; $V$, voltage; $\eta_{ext,max}$, maximum external quantum efficiency; $\eta_{p,max}$, maximum power efficiency; $\eta_{c,max}$, maximum current efficiency; $\eta_{ext}$, external quantum efficiency; $\eta_p$, power efficiency; $\eta_c$, current efficiency. $V_{on}$ was obtained from the $x$-intercept of log(luminance) vs applied voltage plot.

**4**−**6**. Considering the HOMO energy gap between compound **5** and TPBI does not appear to be noticeably larger than that between **2** (or **4**, or **6**) and TPBI, hole leakage to TPBI should not be much different if only the barrier is considered. Because both the barrier and mobility may affect the recombination area, we speculate that compound **5** has a higher hole drift mobility. Although leakage of holes from **acen** to $Alq_3$ significantly shifts the chromaticity of device I away from pure red (vide infra), a BCP layer inserted between **acen** and

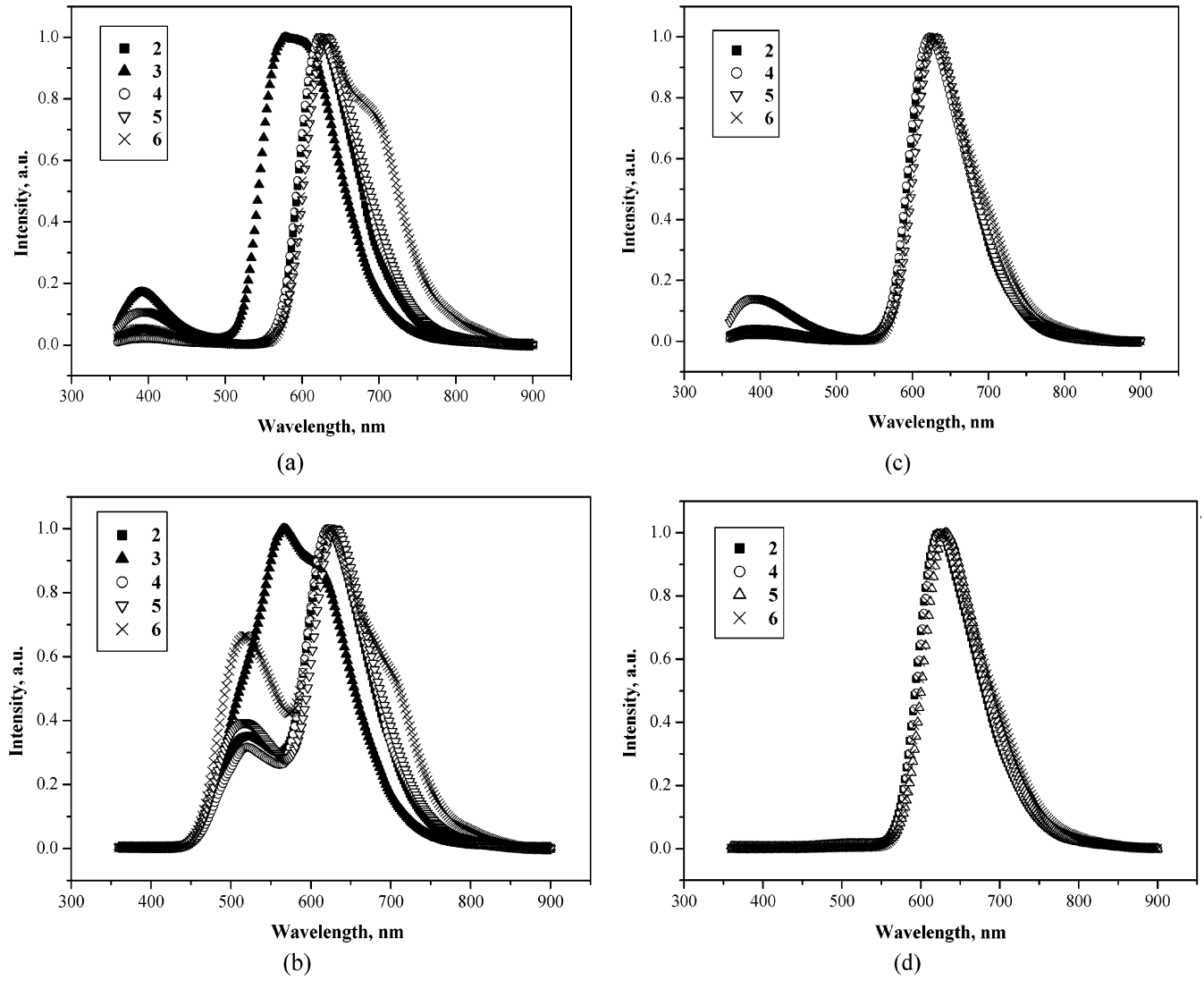


**Figure 7.** EL spectra of the devices I (a), II (b), III (c), and IV (d).

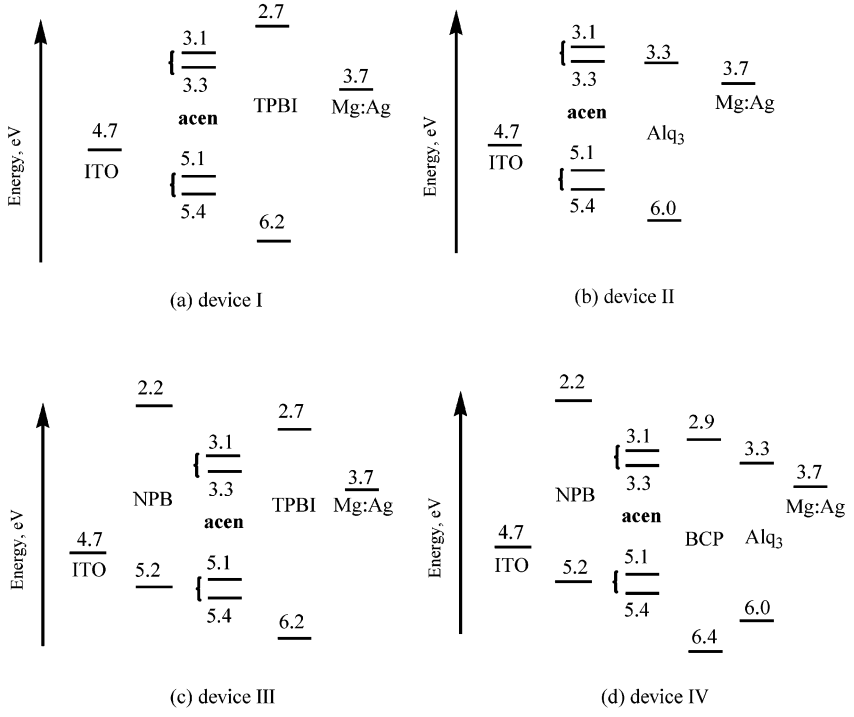


**Figure 8.** Relative energy alignments in the devices I−IV.

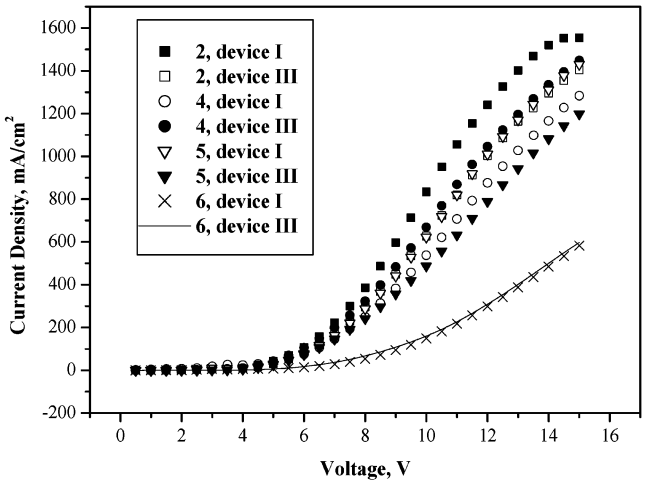


**Figure 9.** Current density vs applied electric field characteristics of the device I vs the device III.

$Alq_3$ completely suppresses the passage of holes out of the **acen** layer in device IV. For each compound, the $I-V$ characteristics of the devices I do not differ much from those of the device III (Figure 9), implying that **acen** has a hole-transporting capability similar to that of NPB. It is not certain whether the variation of the device performance among **acen** reflects their different electron-transporting abilities. The performance of the present devices is inferior to that of some devices using red-dopants reported in the literature, therefore, further modification of the compounds aiming at increasing the fluorescent quantum yields will be conducted. Variation of the peripheral segments and extension to the rubicene system are currently ongoing.

In summary, we have developed a convenient synthesis of high $T_g$ benzo[*a*]aceanthrylene derivatives (**acen**) which are red emitting. Instead of being used as dopant, these compounds can be deposited as thin film, either as a dual functional layer (emitting and hole transporting) or an emitting layer. Pure red-emitting devices can generally be achieved in two-layered devices of the configuration ITO/**acen**/TPBI/Mg:Ag/Ag and the three-layered devices of the configuration ITO/NPB/**acen**/TPBI/Mg:Ag/Ag where TPBI is used as the electron-transporting layer, or in multilayered devices of configuration ITO/NPB/**acen**/BCP/$Alq_3$/Mg:Ag/Ag where BCP and $Alq_3$ were hole-blocking and electron-transporting layers, respectively. When used in conjunction with $Alq_3$ in a two-layer device, fine-tuning of EL emission in the yellow region can be obtained.

**Acknowledgment.** This work was supported by Academia Sinica and National Science Council.

CM034631E